Benjamin Kossack*, Eric L. Wisotzky, Ronny Hänsch, Anna Hilsmann, and Peter Eisert

Local blood flow analysis and visualization from RGB-video sequences

https://doi.org/10.1515/cdbme-2019-0094

Abstract: The extraction of heart rate and other vital parameters from video recordings of a person has attracted much attention over the last years. In this paper, we examine time differences between distinct spatial regions using remote photoplethysmography (rPPG) in order to extract the blood flow path through human skin tissue in the neck and face. We can show that the visualization of the blood flow path corresponds to the physiologically defined path.

Keywords: Blood flow, remote photoplethysmography, cardiovascular, heart rate, pulse transit time.

1 Introduction

The human face is an important source of information about a human being, such as its condition, e.g., measured by the pulse rate, and is therefore used in a variety of different other applications. An optical measuring technique called photoplethysmography (PPG) is commonly used to measure the human pulse rate [1]. The principle of PPG is based on human blood circulation and the fact that blood absorbs more light than surrounding tissue, so variations in blood volume affect light transmission or reflectance accordingly [2]. A PPG sensor placed directly on the skin optically detects these changes in blood volume [2]. Wearing this sensor can cause patients (especially infants and children) to feel uncomfortable and nervous, which can have a negative effect on the measurement. To overcome this, remote photoplethysmography (rPPG) allowing contactless measurements of the pulse rate with a regular camera has been developed [1]. In literature, this method is used to extract the vital parameters globally. Poh et al. [3] present a non-contact, automated, and motion tolerant heart rate measurement from video images based on blind source separation (i.e., independent component analysis). Rapczynski et al. [4] calculate the rPPG signal from the green channel of the subjects skin pixels. In [5], different color spaces are compared to find the best-suited space for human pulse calculation. It is shown that the Hue component in the HSV color space delivers the most accurate pulse rate measurement [5]. De Haan and Jeanne [6] present an algorithm to calculate a chrominance-based rPPG signal. This algorithm works robustly regardless of the subjects skin tone and the color of the illumination with colored light sources (i.e., for nonwhite illumination).

As the heart generates a blood volume pulse (BVP) with each beat, it is the source of blood circulation. The resulting blood flow through the face causes a minimal change in the facial color. The methods of [3–6] estimate the pulse rate by extracting and analyzing the subtle color changes in the skin area (due to the blood circulation). Wu et al. [7] presented a method to make these imperceptible color changes in video recordings visible to the human eye. The method of [7] is noted as Eulerian Video Magnification (EVM).

Since the BVP travels through the body, it causes a volume change inside the arteries. When the heart pumps blood volume into the aorta, it generates a pulse wave [8]. This wave indicates the temporal course and the direction of the flowing blood volume. The pulse transit time (PTT) refers to the time difference between the pulse peaks taken at two arterial sites [9]. After the aorta, the blood flows through several arteries until it reaches the left and right common carotid arteries [8]. The common carotid artery supplies the respective sides of the head and neck and divides into internal and external carotid arteries. The internal carotid artery begins at the carotid sinus and supplies forehead, eyes and part of the nose. The external carotid arteries supply blood to structures within the cheek, lower jaw, neck, and larynx [8]. Figure 1 illustrates which regions of the face are supplied by the external carotid artery and by the internal carotid artery [10].

The aim of this work is to detect and classify vital data locally through human skin tissue from videos to visualize the blood flow and to derive a blood flow path. This work presents a blood flow visualization that can uncover potential regions in the face that are poorly supplied with blood. Besides, intraoperative use of the blood flow visualization is conceivable in order to uncover heavily perfused regions and thus assist the surgeon (e.g., with tissue differentiation).

***Corresponding author: Benjamin Kossack,** Fraunhofer Institute for Telecommunications, Heinrich Hertz Institute, Computer Vision and Graphics Group, Einsteinufer 37, 10587 Berlin, Germany, e-mail: benjamin.kossack@hhi.fraunhofer.de
Eric L. Wisotzky, Anna Hilsmann, Peter Eisert, Fraunhofer Institute for Telecommunications, Heinrich Hertz Institute, Computer Vision and Graphics Group, Berlin, Germany
Ronny Hänsch, Technische Universität Berlin, Computer Vision & Remote Sensing, Berlin, Germany
Eric L. Wisotzky, Peter Eisert, Humboldt-Universität zu Berlin, Visual Computing, Berlin, Germany

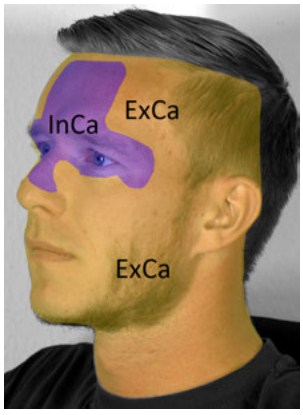

Fig. 1: This figure illustrates areas of the head surface supplied by the internal (InCA) and external (ExCA) carotid arteries [10].

2 Method and Material

2.1 Local rPPG Signal Analysis

The visualization of blood flow is based on a reliable and stable local rPPG signal. We investigate different rPPG signal types locally to identify the most reliable rPPG method for this work. We use the signal-to-noise ratio (SNR) definition by de Haan and Jeanne [6] to quantify the signal quality.

Thus, we compare the local qualities of the resulting signals of *Hue* [5], *Green* (green channel of the RGB color space) [4], G_n (normalized green value) [4], *Independent components* (*ICs*) [3], and *Chro* (chrominance-based) [6]. In contrast to literature, we expanded the calculation and analyze the rPPG signals pixelwise.

A thresholding test is applied to determine the signal quality of each signal type. In order to reduce noise and computational costs, we calculate a Gaussian pyramid for each image of a video recording. We transform the images of the second pyramid level into local representations of *Hue*, *Green*, G_n, *ICs*, and *Chro*. Subsequently, we calculate the SNR for each pixel and perform a binary threshold operation at $0\,\mathrm{dB}$ to determine the signal type that holds the most pixels above that threshold. The results of six randomly selected video sequences of our database are shown in Table 1. The bold highlighted cells in this table mark the signal type with the most pixel positions above $SNR_{th} = 0\,\mathrm{dB}$. The results indicate that the *Chro* signal is the best local rPPG signal representation (from the analyzed signals).

2.2 Extracting Spatial Time Delay

To visualize the blood flow, we need to reveal that the BVP reaches different spatial regions within the face at different times. The time delay between these rPPG signals of different spatial regions is calculated via the phase angles of the pulse frequency component f_{pr} in the frequency domain. After a fast Fourier transform (FFT) is applied to each local signal, we calculate the phase difference of the spatial rPPG signals of interest

$$\Delta\varphi_i(f_{pr}) = \varphi_{ref}(f_{pr}) - \varphi_i(f_{pr}), \tag{1}$$

where $\varphi_{ref}(f_{pr})$ is the phase angle of a reference position and $\varphi_i(f_{pr})$ is the phase angle of a position of interest. Then, the time delay is then calculated by

$$\Delta t_i = \frac{\Delta\varphi_i(f_{pr})}{2\pi f_{pr}}, \tag{2}$$

where f_{pr} is the global pulse frequency. This time difference Δt_i shows that the BVP reaches certain points in the face earlier than other points.

Tab. 1: The number of pixels with an SNR above $0\,\mathrm{dB}$ for each signal type, where each row represents the results for a distinct video recording. For each video sequence, the bold cell indicates the signal type with the most pixel positions above $0\,\mathrm{dB}$.

Video sequence	Number of pixel with $SNR > 0\,\mathrm{dB}$				
	Hue	Green	G_n	ICs	Chro
ID01	8100	7014	9599	9714	**11946**
ID02	4887	2670	4978	4769	**5576**
ID03	3848	3276	3789	4160	**4484**
ID04	6626	3399	7085	7389	**8032**
ID05	12977	7377	13428	12335	**14047**
ID06	1253	253	1286	1229	**1634**

2.3 Data Acquisition

A dataset of 88 video sequences of twelve healthy probands (with age between 25 and 33 years) is created. Each proband is connected to a vital sign monitor (VitaGuard 3100, GETEMED, Germany) to measure the ECG and PPG simultaneously to the video recording. In order to achieve higher robustness against motion artifacts and due to the higher sampling frequency, the ECG measurements are used as reference data in this work. The recorded scene is illuminated by compact daylight ($\approx 5600\,\mathrm{K}$) LED sources. These light sources are placed in front of the subject with an angle of $30°$ to both sides, to reduce shadow on the subject's face. During the data acquisition, subjects are recorded in different positions (frontal and lateral), and with varying heart rate (resting and increased). All subjects reach an increased heart rate through physical activity prior to recording.

2.4 Proposed Framework

To visualize the human blood flow, we applied the framework shown in Figure 2. As in [7], we spatially filter each frame of the input video by calculating a Gaussian pyramid for each frame. In contrast to Section 2.1, we use the images of the third-level of the pyramid to increase the SNR (by reducing noise) and to reduce computational costs. The remaining levels are discarded. As shown in Figure 3, from one of the filtered images, a contour containing face and neck is selected (e.g., with face recognition or manually). After the spatial filtering, we use the normalized green channel [4] to calculate the global pulse rate f_{pr}, as this method leads to satisfying results for all our recordings.

Then, we apply the chrominance-based method [6] to each spatial position to receive the local rPPG signal. We calculate the SNR for the global pulse frequency from the local rPPG signals within the selected face and neck contour. Additionally, we calculate a binary SNR-threshold-mask to include only spatial position providing a reliable rPPG signal.

All positions below a certain threshold SNR_{th} are excluded from further processing. Throughout this work, a segmentation of the visible skin tissue is reached with

$$SNR_{th} = \mu(SNR_{rPPG}) - 2\sigma(SNR_{rPPG}), \qquad (3)$$

where SNR_{rPPG} represents the SNR of all positions within the selected face and neck contour, the operator σ corresponds to the standard deviation, and μ corresponds to the mean. All spatial positions in the SNR-threshold-mask (i.e., the region of interest (ROI)) (see Figure 3), carry the pulse rate of the recorded person and the remaining positions are ignored for further processing.

In this work, we calculate the time difference between signals of different position without any filtering via the phase angles in the frequency domain. Therefore, the FFT for each spatial rPPG signal within the ROI is calculated. We then extract the phase angle $\varphi(f_{pr})$ of the frequency component according to f_{pr}.

In order to remove incorrectly calculated phase angles, we check all angles for plausibility, whereby angles that correspond to time delays of more than $\Delta t_i = 0.3\,\mathrm{s}$ are excluded, as they are physiologically impossible [8]. We select the spatial position with the largest phase angle as the reference point. This point corresponds to the position where the BVP appears last in time. In almost all frontal recordings, the position of the highest phase angle is located near the subject's mouth. To make the measurements of the individual subjects comparable, the reference point φ_{ref} of the PTT map is always selected within a rectangular area centered around the center of the mouth of the subject.

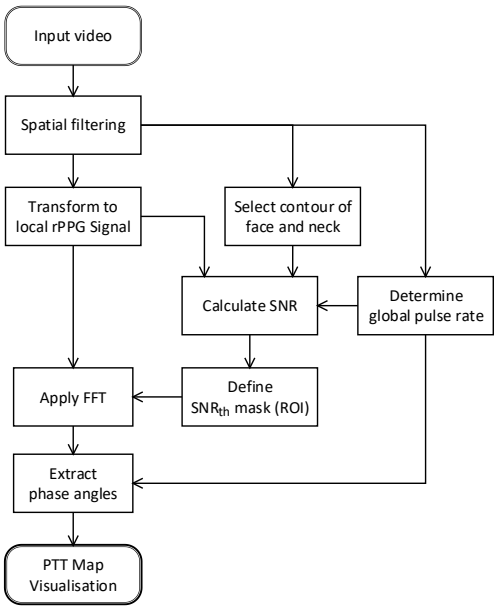

Fig. 2: Overall description of the framework to visualize the blood flow.

In the last step, the phase differences $\Delta\varphi_i$ between the reference position and all other positions are calculated and Equation (2) is applied to convert the resulting phase differences into the time delays Δt_i.

3 Results

We assume that the time delay corresponds to the time difference required by the peak of the BVP to reach different regions and thus corresponds to PTT. Therefore, the visualization of the blood flow is achieved with PTT maps, which map the calculated time delays to their spatial position. Figure 4 shows the resulting PTT maps for recordings of *ID01* and *ID02*.

Fig. 3: This figure shows an arbitrary input frame of *ID01* (after pre-processing), the selected face and neck contour, and the corresponding SNR-threshold-mask (i.e., ROI).

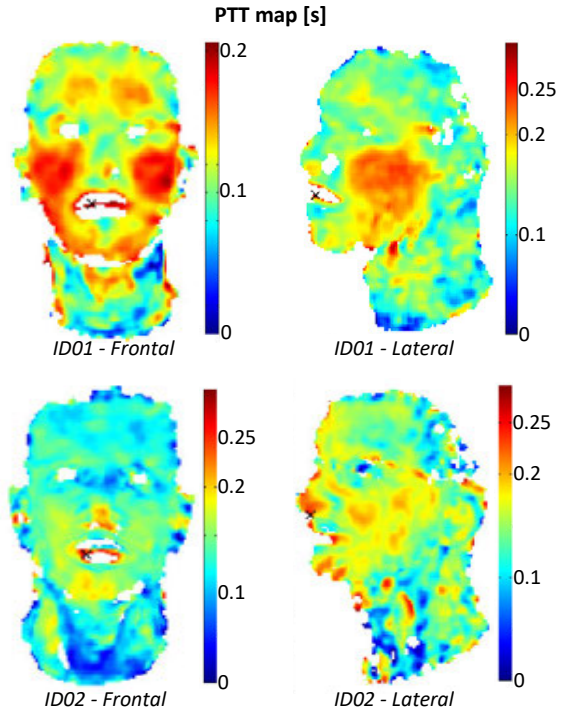

Fig. 4: This figure shows the resulting frontal and lateral PTT maps of *ID01* and *ID02*. The black cross shows the position of φ_{ref}, which is last reached by the BVP.

4 Discussion and Conclusion

We visualize the blood flow through the skin tissue of the neck and head in the form of PTT maps. The analyzed subject data show consistent results and patterns (see Figure 4). Partial coverings of the skin tissue by head hair, beard, and jewelry or poor SNR cause artifacts and exclusions in the time delays.

Figure 4 shows the resulting lateral and frontal PTT maps for two subjects. The color coding of the maps in Figure 4 shows areas in blue where the BVP arrives first and in red where the BVP arrives at a later point in time. The physiological described arterial blood flow path can be found in all PTT maps. The oxygenated blood flows first into the neck and head via the common carotid arteries. The majority of the frontal and lateral PTT maps show a blue region on the neck (see Figure 4). This blue color indicates an area where the pulse appears early compared to the other spatial regions. The blue areas on the neck probably represent the blood that flows through the common carotid arteries into the head. Therefore, it can be concluded that the PTT maps can indicate the position of the common carotid arteries.

Figure 1 shows that the forehead of a human being is supplied by the internal carotid artery and the rest of the face by the external carotid artery. This difference in supply arteries can also be identified in the PTT maps. Each PTT map shows that the pulse peak reaches the forehead earlier than the rest of the face. This delay leads to the conclusion that the external carotid supplies the cheeks, chin, and mouth later with blood than the internal carotid the forehead region.

In this work, the chrominance-based rPPG signal is analyzed locally for the first time in order to visualize the blood flow. From that, we obtain the position of specific arteries, the path of the BVP, and it is possible to extract the PTT. It is conceivable that the presented blood flow visualization can also be used to differentiate between different soft tissues during surgery similarly as in [11, 12]. Besides, analysis with hyperspectral imaging (HSI) and a combination of specific bands could lead to better local rPPG visualization.

References

[1] Zaunseder, S., Trumpp, A., Wedekind, D., Malberg, H. (2018). Cardiovascular assessment by imaging photoplethysmography - A review. Biomedizinische Technik, 1–18.

[2] Tamura, T., Maeda, Y., Sekine, M., Yoshida, M. (2014). Wearable Photoplethysmographic Sensors—Past and Present. Electronics, 3(2), 282–302.

[3] Poh, M.-Z., McDuff, D. J., Picard, R. W. (2010). Non-contact, automated cardiac pulse measurements using video imaging and blind source separation. Optics Express, 18(10), 10762.

[4] Rapczynski, M., Werner, P., Al-Hamadi, A. (2017). Continuous low latency heart rate estimation from painful faces in real time. Proceedings - International Conference on Pattern Recognition, 1165–1170.

[5] Tsouri, G. R., Li, Z. (2015). On the benefits of alternative color spaces for non-contact heart rate measurements using standard red-green-blue cameras. Journal of Biomedical Optics, 20(4), 048002.

[6] De Haan, G., Jeanne, V. (2013). Robust pulse rate from chrominance-based rPPG. IEEE Transactions on Biomedical Engineering, 60(10), 2878–2886.

[7] Wu, H.-Y., Rubinstein, M., Shih, E., Guttag, J., Durand, F., Freeman, W. (2012). Eulerian video magnification for revealing subtle changes in the world. ACM Transactions on Graphics.

[8] Betts, J. G. and others (2017). Anatomy & Physiology, openstax.

[9] i Carós, S., Maria, J. (2011). Continuous non-invasive blood pressure estimation. ETH Zurich.

[10] von Arx, T., Tamura, K., Yukiya, O., Lozanoff, S. (2018). The Face – A Vascular Perspective. A literature review. Swiss Dental Journal, 128(5), 382–392.

[11] Wisotzky, E. L., Uecker, F. C., Arens, P., Dommerich, S., Hilsmann, A., Eisert, P. (2018). Intraoperative hyperspectral determination of human tissue properties. J. Biomed. Opt., 23(9), 091409.

[12] Wisotzky, E. L., Kossack, B., Uecker, F. C., Arens, P., Dommerich, S., Hilsmann, A., Eisert, P. (2019). Validation of two techniques for intraoperative hyperspectral human tissue determination. Proceedings of SPIE, 10951, 109511Z.